Relaxation behavior in a tiling model for glasses

Thomas A. Weber, Glenn H. Fredrickson, and Frank H. Stillinger
AT&T Bell Laboratories, Murray Hill, New Jersey 07974
(Received 26 June 1986)

A Monte Carlo investigation of the equilibrium and kinetic properties of the square tiling model proposed by Stillinger and Weber is presented. By employing a combination of series expansion and simulation methods, accurate approximations for the equilibrium thermodynamic properties are obtained. The model exhibits nonexponential relaxation of the potential-energy autocorrelation function that empirically can be described by the Kohlrausch-Williams-Watts expression. Furthermore, it is shown to possess non-Arrhenius temperature dependence of the average relaxation time for the potential energy. Continuous cooling and heating simulations, as well as finite-temperature-jump experiments, were performed and the results were found to be in qualitative agreement with the behavior of laboratory glass-forming liquids. The kinetic properties of the square-tiling model are compared with those of the two-spin-facilitated model proposed by Fredrickson and Andersen.

I. INTRODUCTION

Supercooled liquids and the glasses they form display a rich variety of thermodynamic and kinetic phenomena.[1] These include cooling-rate dependence of low-temperature properties, hysteresis effects, and strongly nonexponential relaxation functions following mechanical or electrical perturbations. Furthermore, these attributes appear in their quantitative details to be material dependent; that is, behavior in the neighborhood of experimental glass transitions seems to depend in a nontrivial way on the specific nature of the atomic-level interactions involved.

Theorists have responded to the need to organize and explain these observations with a large array of "models."[2-15] These have differed widely in the fundamental level of starting assumptions, credibility of approximations, and qualitative nature of the deductions. Some of the models are purely phenomenological,[12-15] while others attempt to identify relevant atomic or molecular processes which control macroscopic observables in the supercooling and glass-forming regimes. The long-term goal surely is to produce a formalism whereby detailed knowledge about atomic and molecular interactions for any given substance can directly lead to predictions for all of the above-mentioned properties.

This paper is concerned with a less ambitious goal, namely the study of a specific model for supercooling and vitrification. While this model does not presume to connect explicitly to atomic-level details, it nevertheless has the advantage of precision. Available configurational states are clearly identified at the outset, the energies of those states are specified, and an appropriate set of allowed dynamical transitions (and their rates) between those states is postulated. These attributes suffice to allow study of thermal equilibrium and glass-forming properties both by analytical and by simulational techniques.

The following Sec. II motivates and defines our "tiling model," and stresses that it can be used in principle to examine the kinetic competition between crystallization and vitrification. Section III considers the canonical partition function for the tiling model, and discusses the natural series expansion for the limit in which $\beta=(k_B T)^{-1}$ goes to minus infinity; it also examines the condensation transition that in principle would occur (to a lowest-lying amorphous state) if equilibration continued to obtain at low temperature. Section IV provides details about the Monte Carlo program that has been constructed and applied to study of the model. Section V presents equilibrium results determined by the Monte Carlo simulation in the high-temperature regime, and uses them to locate the putative (but unrealizable) condensation point. Rate processes and relaxation behavior as revealed by the simulation supply the subject in Sec. VI. The closing Sec. VII summarizes conclusions and discusses their implications.

II. TILING MODELS

A brief description of the tiling models has appeared in a prior publication.[16] We now provide a more detailed exposition.

A central underlying concept is that any configuration of particles in a condensed phase can uniquely be referred to a discrete set of mechanically stable packings. This is effected by means of a (mass-weighted) steepest descent on the relevant potential energy hypersurface.[17] For liquids and glasses the resulting packings are amorphous. We shall adopt the point of view here that vibrational deformations away from the stable packings (potential minima) are only incidental to the task of specifying system configurations as they relate to supercooling and vitrification. Instead it should suffice simply to classify packings.

Previous theoretical and simulational studies of simple models for atomic substances show that their amorphous packings display substantial variability in local coordination geometry, local stress, and local bond energy.[18] Some regions are occupied by well-coordinated atoms, others less so. We shall assume that any amorphous packing can be divided into domains of various sizes, the interiors of which contain only well-coordinated, well-bonded particles. Boundaries between contiguous domains then

 ©1986 The American Physical Society

represent locations of strained and weakened bonds, present perhaps because the steric requirements of strong bonding within domains have created geometric frustrations.

In principle the amorphous packing might consist of just a single macroscopic domain. In this event the constituent particles would have discovered one of the lowest-energy noncrystalline packings possible, which is substantially devoid of poor coordination and bonding. For some materials (such as Al-Mn alloys) this might entail quasicrystalline order.[19]

Our model is intended to represent qualitatively the statistical mechanics of the fitting together of collections of domains, and of the kinetics of interconversions between distinct domain patterns. Several drastic simplifications are demanded at the outset for conceptual and computational manageability. We assume the following.

(i) The system is two dimensional.

(ii) Domains are square, and fit without gaps or overlap onto a square lattice with unit spacing (i.e., domain vertices are coincident with points of the lattice).

(iii) All domain sizes $n \times n$ ($n = 1,2,3,\ldots$) are permitted.

(iv) Periodic boundary conditions apply.

Figure 1 shows a typical arrangement of square domains, a "tiling" of the plane, that is consistent with these restrictions.

The potential energy Φ to be assigned to any tiling is equal to the total length of interdomain boundary times λ, a positive energy per unit length of such boundary. We can express Φ succinctly as follows:

$$\Phi = 2\lambda \sum_{j \geq 1} j n_j \ , \tag{2.1}$$

wherein n_j stands for the number of $j \times j$ domains present in the tiling. Since the total area of the system is fixed (equal, say, to N elementary units of area defined by the underlying square lattice), we must have the linear constraint

$$\sum_{j \geq 1} j^2 n_j = N \ . \tag{2.2}$$

The maximum value for Φ is achieved when the tiling consists entirely of 1×1 domains. The minimum value for Φ requires eliminating as much domain boundary as possible; in a square system with periodic boundary conditions this is attained with a single system-spanning domain. The corresponding limits on Φ are

$$2\lambda N^{1/2} \leq \Phi \leq 2\lambda N \ . \tag{2.3}$$

It is easy to show that the difference in Φ values for any two tilings is always a multiple of 4λ.

The set of allowed transitions must be consistent with ergodic behavior. That is, any tiling should be kinetically accessible from any other by a finite sequence of positive-rate transitions. At the same time, the allowed transitions should be sufficiently sparse to guarantee that the system manifest glasslike behavior at low temperature. We want the system under cooling conditions to become inevitably trapped in configurations with Φ substantially above the lower limit specified by Eq. (2.3).

The transitions allowed in the present model either cause the fragmentation of a larger square into smaller ones, or cause the reverse process that aggregates a cluster of smaller squares into a larger one. Specifically we permit a square domain of size $(pq) \times (pq)$ to fragment into a square cluster of p^2 $q \times q$ domains if and only if p is the smallest prime factor of pq. Inversely, a square arrangement of p^2 domains, all of size $q \times q$, can aggregate to form a single $(pq) \times (pq)$ domain, provided that p is the smallest prime factor of pq. These are the *only* allowed processes.

It is clear that this selection yields ergodicity. Any two tilings individually are connected to the fully fragmented state (all 1×1 domains) by a sequence of single-domain fragmentations. Therefore, they are kinetically connected to each other.

The specific form to be used for the allowed aggregation rate is[16]

$$r_a(pq) = \nu_0 \alpha^{2pq(p-1)} \ . \tag{2.4}$$

The factor ν_0 is a fixed attempt frequency that establishes the natural time unit. The parameter α lies in the range

$$0 < \alpha < 1 \ ; \tag{2.5}$$

it is raised to a power equal to the total length of domain wall that would be annihilated by the aggregation process and so acts to reduce the rate strongly when that length is large. The requirement of detailed balance demands that the fragmentation rate be

$$r_f(pq) = r_a(pq) \exp(-\beta \Delta\Phi), \quad \beta = (k_B T)^{-1} \tag{2.6}$$

where $\Delta\Phi$ is the potential energy change produced by the insertion of new domain boundary:

$$\Delta\Phi = 2\lambda pq(p-1) \ . \tag{2.7}$$

The configurational trapping necessary to produce glasslike behavior in the model is assured by this selection

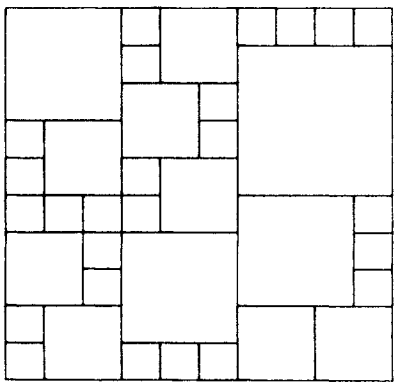

FIG. 1. Typical tiling of the plane with square domains of integer size $n \times n$.

of transitions and rates. As temperature declines, a system at equilibrium would have to exhibit larger and larger squares to lower its energy. However, this becomes increasingly difficult. Not only do the basic aggregation rates in Eq. (2.4) become small for large domains, but also it becomes increasingly unlikely that a preexisting proper arrangement of square domains, all of the same size and in proper registered contact, be found to permit aggregation.

Before proceeding to discuss properties of the model defined in Eqs. (2.1) and (2.4)–(2.7), we remark that a straightforward extension can be implemented which includes the possibility of nucleation and freezing into the crystal, as a process in competition with supercooling and vitrification. We have already identified the interiors of large domains as well-bonded but normally amorphous. A periodic crystal however could formally be identified with a periodic array of domains of some special size, say $a \times a$, each one of which contains some integer number of crystal unit cells instead of amorphous arrangements of atoms. A new term then needs to be incorporated in Φ in Eq. (2.1) to make the array of registered $a \times a$ tiles the system's lowest-energy configuration. Specifically we can take[16]

$$\Phi' = 2\lambda \sum_{j \geq 1} j n_j - \mu a N_{aa} , \tag{2.8}$$

where N_{aa} represents the number of $a \times a$ tiles which are in full contact along a common side. If $\mu > \lambda > 0$, the unfavorable domain-wall energy present in the first part of Φ will be overcome by the new term in the designated "crystal" configuration, but if μ exceeds λ only very slightly the driving force for crystallization will be small.

In any case we see for the tiling models that crystallization and vitrification tendencies logically are not directly connected, but represent distinct aspects of the model which can be separately varied. For the remainder of this paper we consider only the unadorned interaction, Φ in Eq. (2.1).

III. PARTITION FUNCTION

When conditions permit attainment of thermal equilibrium, the configurational free energy F becomes relevant. It can be obtained from the canonical partition function Z:

$$Z(\beta) = \exp(-\beta F) = \sum_{\text{tilings}} \exp(-\beta \Phi) . \tag{3.1}$$

In view of the fact that Φ in Eq. (2.1) depends so simply on the numbers n_j of domains of various sizes, it is useful to rewrite Z as a sum over sets of those numbers subject to the constraint (2.2):

$$Z(\beta) = \sum_{\{n_j\}} \Omega(\{n_j\}) \exp[-\beta \Phi(\{n_j\})] . \tag{3.2}$$

Here Ω stands for the number of distinct tilings that are possible with the given population of tiles.

In contrast to many statistical-mechanical models of cooperative phenomena, the tiling model does not reduce to triviality at infinite temperature ($\beta = 0$). In that limit the Boltzmann factor in Eq. (3.2) can be disregarded, and Z reduces to the total number of distinct tilings. Evidently a precise evaluation of this number remains a major mathematical challenge.

Fortunately the model does have a useful simplifying limit as β, or more precisely $\beta\lambda$, approaches $-\infty$ along the negative real axis. In this limit the partition function will be dominated by the single configuration with maximum Φ, the fully fragmented 1×1 structure. It was remarked earlier that Φ changes in multiples of 4λ. With periodic boundary conditions there are N equivalent tilings, with a single 2×2 in a background of 1×1's, that lie 4λ below the Φ maximum. Tilings with a pair of 2×2's lie 8λ below the maximum, and number $N(N-9)/2$.

By extension of this ordered enumeration scheme it is possible to generate an expansion for the free energy F that is appropriate for the $\beta\lambda \to -\infty$ limit. We find

$$\beta F(\beta)/N = 2\beta\lambda - x + \tfrac{9}{2}x^2 - \tfrac{100}{3}x^3 + O(x^4) , \tag{3.3}$$

where

$$x = \exp(4\beta\lambda) \tag{3.4}$$

is the natural expansion variable. From this series we obtain

$$\langle \Phi \rangle / N\lambda = d(\beta F/N)/d(\beta\lambda) , \tag{3.5}$$

$$\langle \Phi \rangle / N\lambda = 2 - 4x + 36x^2 - 400x^3 + O(x^4) . \tag{3.6}$$

The series (3.3) shows that $\beta F/N$ is strongly negative in the limit $\beta\lambda \to -\infty$, but is increasing as $\beta\lambda$ increases toward zero. From the partition function itself, Eq. (3.2), and Eq. (3.5), we see that $\beta F/N$ is still negative and increasing at $\beta\lambda = 0$. Approximate evaluations of the partition function[16] imply that $\beta F/N$ continues to increase for positive $\beta\lambda$ until it vanishes (still with positive slope) at some critical value $(\beta\lambda)_c$. If indeed the exact free energy has that behavior, then at this point the domain structure of the system would become unstable with respect to expulsion of domain walls from the system's interior. The system then would condense into a single macroscopic amorphous domain if transition rates were to so permit. This single domain configuration has, on a per-unit-area basis, both vanishing energy and vanishing entropy. Simulation results presented below show indeed that this condensation point exists, just as suggested by the approximate theory.[16]

IV. MONTE CARLO SIMULATION

The Monte Carlo simulation of glasses presents an intrinsically formidable problem because as the temperature is lowered, longer and longer runs are needed to reach equilibrium. In the standard Metropolis Monte Carlo formulation,[20] the probability of rejection of moves also increases dramatically at lower temperatures and compounds the inherent equilibration problem. To overcome this latter difficulty an algorithm of the genre proposed by Bortz, Kalos, and Lebowitz[21] was developed for the simulations.

The algorithm is constructed by determining all of the

possible transitions out of the system's momentary configuration, either by aggregation or by fragmentation, for each of the qualifying squares. Each such square will have a characteristic transition rate, and for aggregation this depends upon its local environment. The sum of all of the individual transition rates for these parallel processes yields the total transition from the given configuration

$$R = 1/\Delta t = \sum_{\text{squares}} r_{\text{square}} . \tag{4.1}$$

Here Δt is the expected lifetime of the configuration. A random number between 0 and R is then generated to determine which of the possible transitions is to be effected. In this algorithm every Monte Carlo move changes the system's configuration. The elapsed time is calculated by summing all of the Δt's for the sequence of preceding configurations.

As remarked earlier, the inverse of the attempt frequency ν_0 appearing in aggregation and fragmentation rate expressions (2.4) and (2.6) supplies a natural time unit for the simulation. Furthermore, the parameter α also appearing in those expressions was given the value

$$\alpha = 0.98 \tag{4.2}$$

in all of the calculations reported in this paper.

Accounting for all possible fragmentation processes that could alter a given configuration is simple; each square tile can divide into smaller tiles only in the one way specified by the smallest prime factor of its side length. Thus a 2×2 can only fragment into four 1×1's, a 3×3 can fragment only into nine 1×1's, a 4×4 only into four 2×2's, etc.

By contrast, it is far less straightforward to identify all possible aggregations that might befall a given configuration. Square clusters of equal-sized and registered tiles must be located, of course. But the aggregation rule specified in Sec. II above only permits some of these to create a larger tile. For example, clusters of 5×5 tiles are only allowed to form tiles of size 10×10, 15×15, or 25×25.

After a transition has been made, the old and new configurations will normally differ only by a localized geometric change. Consequently many of the possible transitions and their rates calculated for the old configuration will continue to apply to the new configuration. However, scrupulous attention must be devoted to altering the transitions and rates in the neighborhood of the localized change.

Extensive Monte Carlo calculations have been carried out on two system sizes, 50×50 and 100×100 (i.e., $N=2500$ and 10000). Both positive and negative values of the inverse temperature parameter $\beta\lambda$ have been investigated. When $\beta\lambda \lesssim 0.25$, equilibration can be reproducibly achieved, and the average energies per unit area for the two system sizes (where comparisons have been made) typically agree to within 0.5%. Simulations in both cases were started with uniform arrangements of 2×2 tiles, then equilibrated at high temperature. Lower temperature runs were initiated with final configurations of preceding runs, then equilibrated. Both static and dynamic properties were then evaluated after initial relaxation periods had elapsed at the temperature of interest.

V. ENERGY, ENTROPY, AND THE CONDENSATION POINT

The series expansion results of Sec. III can be combined with Monte Carlo simulation data, obtained in the manner described in Sec. IV, to provide an accurate approximation for the average potential energy function of the square model. This potential energy expression can then be used to obtain accurate approximations for the entropy and free energy. Estimates of the condensation temperature and the number of possible tilings follow.

We have developed a very accurate [3/3] Padé approximant[22] for $\langle\Phi\rangle/N\lambda$ by combining the first three nontrivial coefficients in the expansion of Eq. (3.6) with three equilibrium data points obtained by Monte Carlo simulation at temperatures given by $\beta\lambda=-0.10$, 0.10, and 0.25. The values of the potential energy at these temperatures are reproducible and are believed to reflect true thermodynamic equilibrium. The simulation data are listed in Table I. By solving a system of three linear equations for the three unknown coefficients, the following approximant is obtained:

$$\frac{\langle\Phi\rangle}{N\lambda} = \frac{2+28.26x+69.73x^2-1.840x^3}{1+16.13x+49.12x^2+6.995x^3} , \tag{5.1}$$

where x is defined above in Eq. (3.4). This approximation for the potential energy function is in excellent agreement with all the Monte Carlo data for $\beta\lambda \lesssim 0.25$. Figure 2 provides a comparison with the simulation results. The poles of Eq. (5.1) are found all to lie on the negative real x

TABLE I. Mean values of the potential energy for the tiling model at various temperature. Values above the solid line refer to well equilibrated Monte Carlo runs. Those below the solid line are metastable states resulting from very slow cooling below the ideal glass transition temperature at $\beta\lambda=0.268$.

$\beta\lambda$	$\langle\Phi\rangle/N\lambda$
−0.30	1.598
−0.20	1.522
−0.10	1.437
−0.05	1.392
0.00	1.342
0.05	1.280
0.10	1.225
0.15	1.170
0.20	1.092
0.25	1.015
0.30	0.890
0.35	0.716
0.40	0.593
0.45	0.486
0.50	0.440
1.00	0.409
10.00	0.405

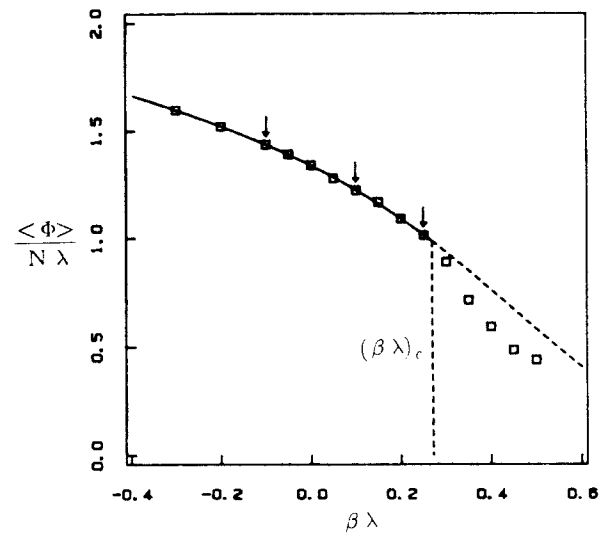

FIG. 2. Comparison of the Monte Carlo data (squares) for the average potential energy of the square model with the Padé approximant (solid curve) given in Eq. (5.1). The agreement is seen to be excellent above the condensation temperature $(\beta\lambda)_c$, but the analytic continuation of the Padé to below the transition (dashed curve) differs significantly from our (nonequilibrium) simulation data.

axis, at -6.681, -0.2595, and -0.08247. The magnitude of the last of these provides an estimate of the radius of convergence of the original series, Eq. (3.6).

Equation (5.1) can be used to obtain the free energy and entropy of the square model by making use of the relations

$$\frac{\beta F}{N}=2\beta\lambda+\int_{-\infty}^{\beta\lambda}[\langle\Phi\rangle/N\lambda-2]d(\beta\lambda)' , \tag{5.2}$$

$$\frac{S}{k_B N}=-\frac{\beta F}{N}+\beta\lambda[\langle\Phi\rangle/N\lambda] . \tag{5.3}$$

We have numerically integrated the first of these equations to obtain $\beta F/N$ and $S/k_B N$ as functions of $\beta\lambda$. Figure 3 shows the behavior of the free energy for the temperature range $-0.1\leq\beta\lambda\leq 0.3$. The free energy is seen to be a monotonically increasing function of $\beta\lambda$ with positive slope and slightly negative curvature. At a critical value of $(\beta\lambda)_c=0.268$ the approximation predicts that the free energy vanishes and hence locates the temperature of the condensation transition described in Sec. III.

The entropy of the square model is also found to be a smooth function of $\beta\lambda$ and is shown in Fig. 4. Its maximum value occurs at infinite temperature ($\beta\lambda=0$) and can be used to obtain an estimate of the total number of possible tilings. We find the result

$$\Omega_{\text{tot}}\sim\exp(0.3155N) . \tag{5.4}$$

The predictions of Eqs. (5.1)–(5.4) for the location of the condensation temperature and the number of tilings are believed to be quite accurate. It is of interest, however, to compare these results with the predictions of the simple Flory approximation and the "improved" Flory approximation presented earlier.[16] These earlier results for the location of the condensation transition were based on the criterion that the quadratic exponents in the concentrations of microscopic square sizes vanish in the approximations, not on the present criterion that the free energy vanish. Of course, in an exact theory both criteria must lead to the same answer, but in the mean field theories the predictions differ. If we insist on the criterion that the free energy must vanish at the condensation point, the mean-field approximations provide the following estimates for the location of the transition:

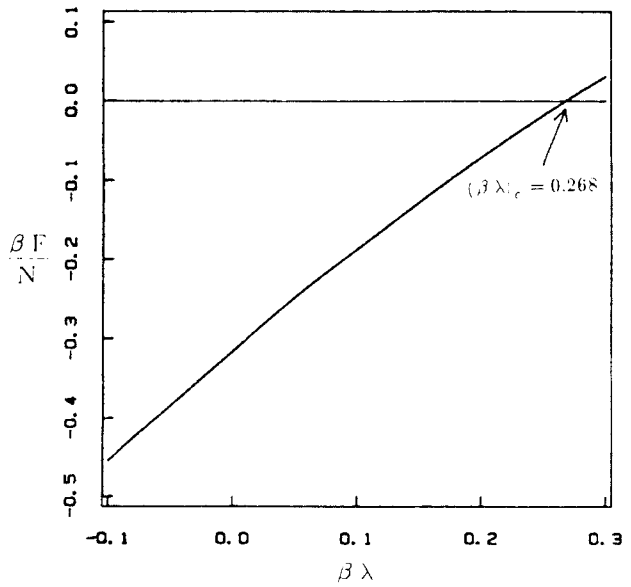

FIG. 3. The free energy for the square model as a function of $\beta\lambda$. The vanishing of the free energy at $\beta\lambda=0.268$ signals the condensation transition.

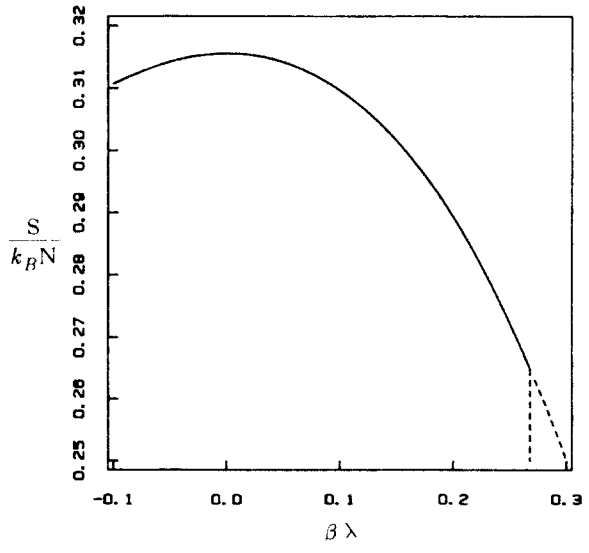

FIG. 4. The entropy of the square model obtained from Eq. (5.3). The maximum at $\beta\lambda=0$ provides an estimate of the total number of tilings in the model [Eq. (5.4)].

$$(\beta\lambda)_c = 0.3260 \quad \text{(Flory)}, \tag{5.5}$$

$$(\beta\lambda)_c = 0.2315 \quad \text{(improved Flory)}. \tag{5.6}$$

These predictions are seen to bound our more accurate estimate of $(\beta\lambda)_c = 0.268$. The corresponding estimates for the total number of tilings are:

$$\Omega_{\text{tot}} = \exp(0.2437N) \quad \text{(Flory)}, \tag{5.7}$$

$$\Omega_{\text{tot}} = \exp(0.2989N) \quad \text{(improved Flory)}. \tag{5.8}$$

For both the location of the transition and the number of tilings the improved Flory approximation is in reasonably good agreement with our more accurate results based on Eqs. (5.1)–(5.3).

Because of the excellent fit of the Padé approximant to the simulation data for the potential energy function and the seemingly smooth behavior of the free energy in the vicinity of $\beta\lambda = 0.268$, it is difficult to imagine that an exact analysis of the partition function in Eq. (3.2) would fail to yield a thermodynamic phase transition.

VI. RATE PROCESSES AND RELAXATION

At temperatures above the predicted condensation transition ($\beta\lambda \leq 0.268$) we were able to equilibrate the model reproducibly in our computer simulations, either by starting from the state with all 2×2 squares, or from some previously equilibrated state of the system at a different temperature. At temperatures below the condensation temperature, the thermodynamically stable state is the state containing a single $N^{1/2}\times N^{1/2}$ square and we were never able to attain this configuration during our simulations. The time required even to equilibrate the smaller system with area 2500 below the transition is astronomically large, and indeed the equilibration time becomes infinite as the size of the system approaches infinity. As a result, the square model possesses an *ideal* glass transition at the condensation temperature $(\beta\lambda)_c$ that is a consequence of an underlying first order phase transition. Because structural relaxation times diverge at $(\beta\lambda)_c$, on cooling at a finite rate we expect to observe failure to attain equilibrium at temperatures even above the ideal transition.

In an attempt to observe such "laboratory glass transitions" in the square model we have performed a series of continuous cooling experiments on the computer. The simulations were carried out on the smaller system with area 2500 that was fully equilibrated at $\beta\lambda = 0.05$. For convenience we define a dimensionless temperature as $T = 1/\beta\lambda$ and express all cooling rates in terms of the dimensionless ratio $\gamma = dT/dt$, where the time t as usual is in units of ν_0^{-1}. Starting from an equilibrium configuration at $T = 20.0$, the system was continuously cooled at rates corresponding to $\gamma = 1.0$, 0.2, 0.02, and 0.002. The cooling program was continued down to a temperature of 0.3 and for each cooling rate the potential energy was monitored as a function of temperature. A series of independent cooling runs was performed for each rate and these were averaged to obtain smoothed data for the potential energy.

Figure 5 shows the results of the continuous cooling experiments. As expected, the system could follow the prescribed temperature program, remaining in equilibrium, to lower temperatures for the slower cooling rates. At the fastest cooling rate, $\gamma = 1.0$, the system fell out of equilibrium (i.e., passed through a laboratory glass transition) at a very high temperature, $T_g \approx 10$. For the slowest cooling rate, $\gamma = 0.002$, the system was able to remain in equilibrium until finally undergoing a glass transition at $T_g \approx 4$. The qualitative features of the behavior seen in Fig. 5 for the square model are in agreement with experiments (such as differential scanning calorimetry) on real

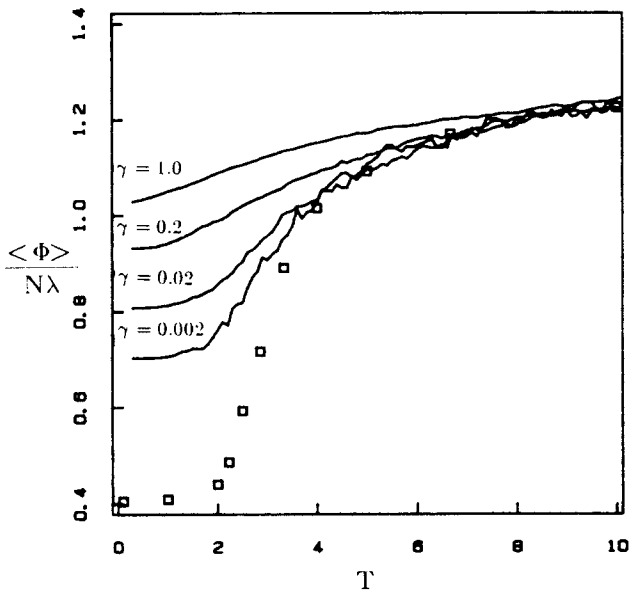

FIG. 5. Dependence of the potential energy on the rate of cooling. The solid curves correspond to cooling rates of $\gamma = 1.0$, 0.2, 0.02, and 0.002. The squares were obtained by the procedure described in Sec. VI.

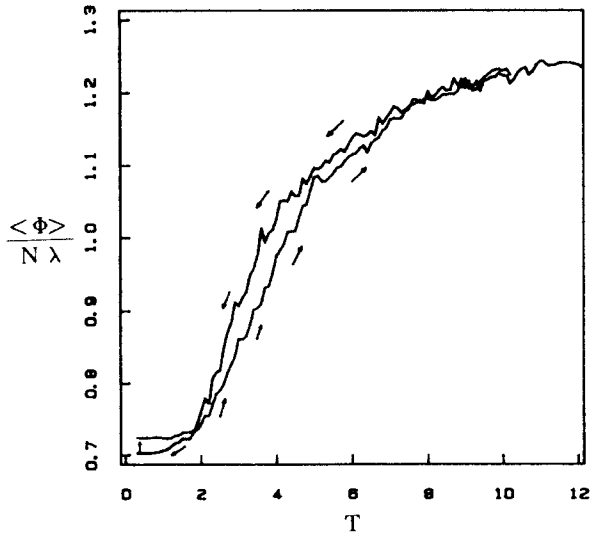

FIG. 6. Hysteresis in the square tiling model. The upper curve corresponds to cooling at a rate $\gamma = 0.002$. After annealing at $T = 0.3$ for a time of 1.8×10^4, the system was reheated at the same rate.

glass-forming materials.[1]

The open squares in Fig. 5 are the result of an extremely slow, stepwise, nonuniform cooling schedule. For each point, the larger 100×100 system was "aged" for one hour on a Cray XMP computer, and then a subsequent hour was utilized to obtain the reported average. At $\beta\lambda=0.10$, 1.6×10^5 moves occurred per simulation hour, while at $\beta\lambda=0.50$, 1.1×10^6 moves occurred per hour.

The square model also exhibits hysteresis on reheating from temperatures below the ideal transition. Figure 6 illustrates the result of cooling the model from $T=20$ to 0.3 at a rate of $\gamma=0.002$, annealing at $T=0.3$ for a time of 1.8×10^4, and reheating to $T=10$ at a rate of $\gamma=0.002$. The increase in potential energy during the annealing stage is a result of the scarcity of allowed transitions that could take the nonequilibrium system to states of lower potential. Figure 7 shows the configuration of the area=2500 system following the cooling stage at $T=0.3$. Because of the significant population of large squares and their random placements, very few transitions can occur in the system that will lower the amount of boundary and hence the energy. (For contrast, Fig. 8 shows a typical configuration from equilibrium at $\beta\lambda=-0.20$.) Instead, during the relatively short annealing time that was imposed the system underwent a fluctuation to higher energy states via the more available fragmentation transitions. On reheating the system, Fig. 6 shows the hysteresis often observed for laboratory glasses—the heating curve falls below the cooling curve. At a temperature of about $T=8$, significantly above the condensation point, the heating and cooling curves merge with the equilibrium potential energy curve.

A second type of experiment that clearly illustrates the nonlinear response of viscous liquids and glasses to finite perturbations is the measurement of the time-dependent response of a material to a pair of finite temperature jumps equal in magnitude, but opposite in sign.[23] We have performed such experiments for the square model, staring the system from an equilibrium configuration at $T=10$ and from the lowest energy configuration we could attain at $T=3$ (i.e., following the procedure described above for the dashed curve in Fig. 5). For each of the two starting configurations, the area=2500 system was instantaneously quenched or heated to a final temperature of $T=6.5$. By monitoring the potential energy as a function of time after this event, we obtained the nonlinear response of the square model to temperature jumps equal in magnitude, but opposite in sign.

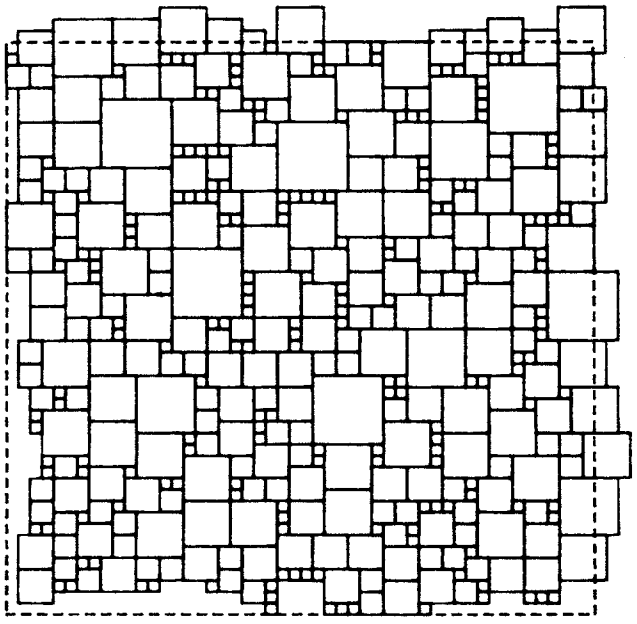

FIG. 7. The $T=0.3$ configuration of the area=2500 system following the cooling program depicted in Fig. 6.

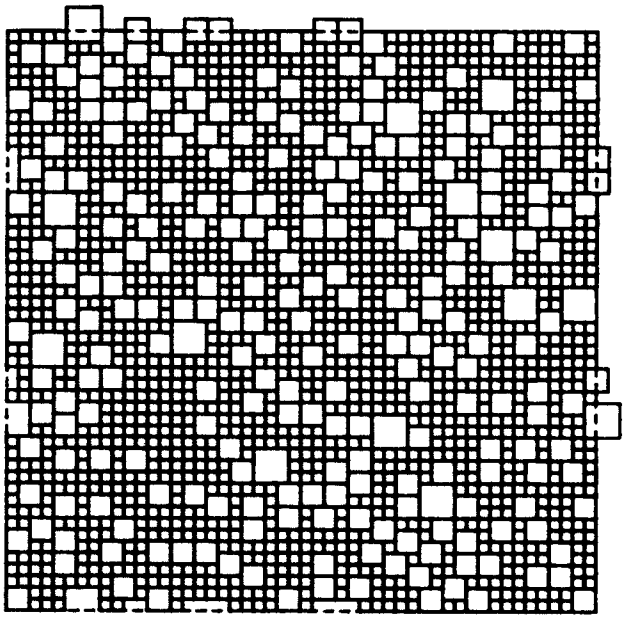

FIG. 8. Typical configuration of the area=2500 system equilibrated at $\beta\lambda=-0.20$. Note the finer texture compared to that in Fig. 7.

Figure 9 illustrates the result of the above experiment. The upper curve represents the average of ten independent quenches from $T=10$ to 6.5 and the lower curve is the result of averaging ten independent quenches from $T=3$ to 6.5. The marked asymmetry of the response is typical of real materials and reflects the fact that strongly cooperative systems require longer to equilibrate when prepared from a low temperature, than from a high temperature. For the experiment depicted in Fig. 9, the time for half the change of the potential energy to occur for the lower starting temperature is twenty times that for half of the change from $T=10$ to occur.

In addition to the nonlinear aspects of relaxation in the square tiling model, we have investigated its linear dynamical response through evaluation of the potential energy autocorrelation function at equilibrium, defined by

$$\phi(t)=\frac{\langle\Phi(t)\Phi(0)\rangle-\langle\Phi\rangle^2}{\langle\Phi^2\rangle-\langle\Phi\rangle^2}\ . \tag{6.1}$$

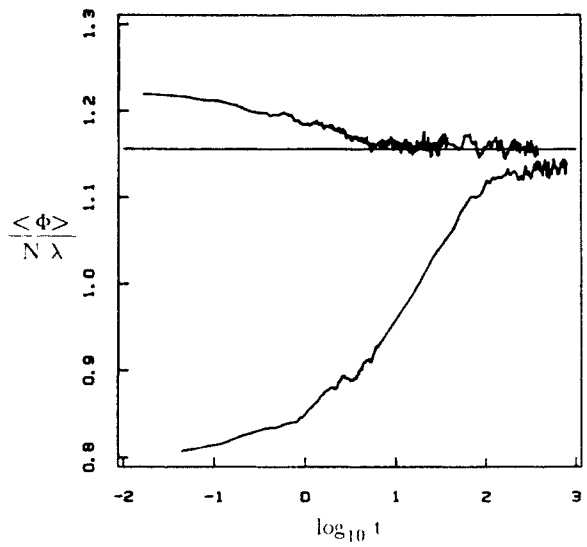

FIG. 9. Asymmetry in the relaxation behavior of the square tiling model. The upper curve describes the response of the model to an instantaneous temperature jump from $T=10$ to 6.5. The lower curve describes the response of the model to a temperature jump equal in magnitude, but opposite in sign, from $T=3$ to 6.5.

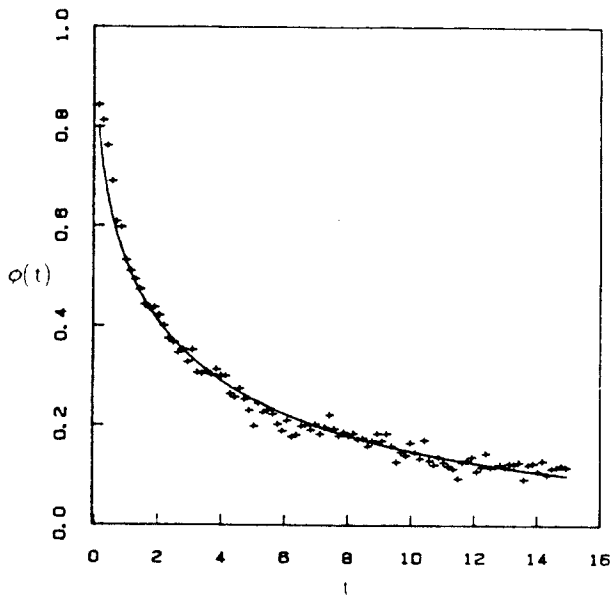

FIG. 11. Potential-energy autocorrelation function at $\beta\lambda=0.10$. The solid line through the Monte Carlo data is a fit to the KWW function with parameters $\mu=0.48$ and $\tau_w=2.5$.

The calculation of this autocorrelation function turns out to be computationally intensive, but we have been able to obtain its short to intermediate time decay with reasonable accuracy for temperatures in the range $-0.1\leq\beta\lambda\leq 0.1$. At each temperature the system was first prepared by performing a run of sufficient length to ensure thermodynamic equilibrium. The final configuration at the end of the run was used to start a new simulation run in which 4×10^4 configurations of the system were saved and whose total length was approximately 100 times the average relaxation time at the appropriate temperature. The potential energy autocorrelation function was computed from the chain of saved configurations. The correlation functions obtained in this manner were fitted to the Kohlrausch-Williams-Watts (KWW)[24] function

$$\phi(t)=\exp[-(t/\tau_w)^{\mu}] , \tag{6.2}$$

where τ_w and μ are adjustable parameters. In obtaining these fits, only data points were used for which $\phi(t)$ had decayed to below 0.5 and no data points were used beyond the first point at which the numerical autocorrelation displayed a negative value.

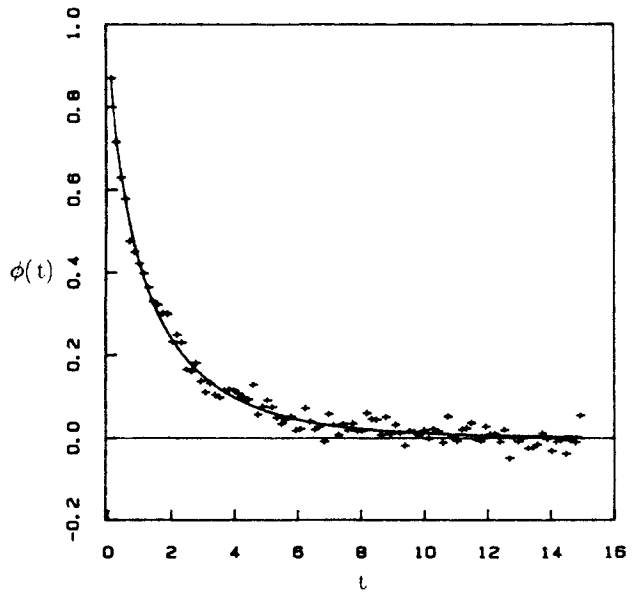

FIG. 10. Potential-energy autocorrelation function (normalized) at $\beta\lambda=0.05$. The solid line through the Monte Carlo data is a fit to the KWW function with parameters $\mu=0.71$ and $\tau_w=1.2$.

Figures 10 and 11 show the simulation data and the KWW fits for the energy autocorrelation function at the two positive temperatures investigated. In both cases the fits are seen to be reasonably good and the values of the exponent μ obtained, 0.71 and 0.48, respectively, indicate that the data could *not* have been fitted by a single exponential. Observation of nonexponential linear response functions that can be described by Eq. (6.2) is a characteristic feature of glass-forming liquids at low temperatures.[23,24]

The values of the KWW parameters for the temperatures investigated in the present study are listed in Table II. The exponent μ is very sensitive to noise in the data, so at best we can only expect to extract qualitative trends shown by the data in Table II. It is apparent, however, that μ is certainly less than unity over this temperature range and that it appears to be decreasing slightly as the temperature is lowered. This lack of thermorheological simplicity is often found in experimental systems and has

TABLE II. Kohlrausch-Williams-Watts parameters for the potential-energy autocorrelation function.

$\beta\lambda$	τ_w	μ	τ
−0.10	0.14	0.81	0.16
−0.05	0.24	0.74	0.29
0.0	0.60	0.85	0.65
0.05	1.2	0.71	1.5
0.10	2.5	0.48	5.6

also been observed in computer simulations of the facilitated kinetic Ising models.[11,25] Table II indicates that the KWW parameter τ_w is much more strongly temperature dependent than μ and consistently increases as the temperature is lowered. The characteristic relaxation time τ shown in the table is defined as the area under the fitted KWW function and is related to τ_w and μ by $\tau=\tau_w\mu^{-1}\Gamma(\mu^{-1})$.

As $\beta\lambda$ increases toward the ideal glass transition point, it becomes increasingly difficult to fit the energy autocorrelation function to the KWW form. The appendix indicates one reason for such behavior, namely that the asymptotic behavior for long times apparently involves an algebraic decay. Consequently the KWW function, however convenient as a fitting device, probably has no fundamental significance for the present class of tiling models.

Figure 12 is an Arrhenius plot of the average relaxation time τ for the square model. The activation energy is clearly a decreasing function of temperature, in agreement with the behavior of viscous liquids near their glass transition.[1,23] It is of interest to attempt a fit of the Adam-Gibbs equation[2] to the entropy and relaxation time data shown in Figs. 4 and 12. The Adam-Gibbs hypothesis

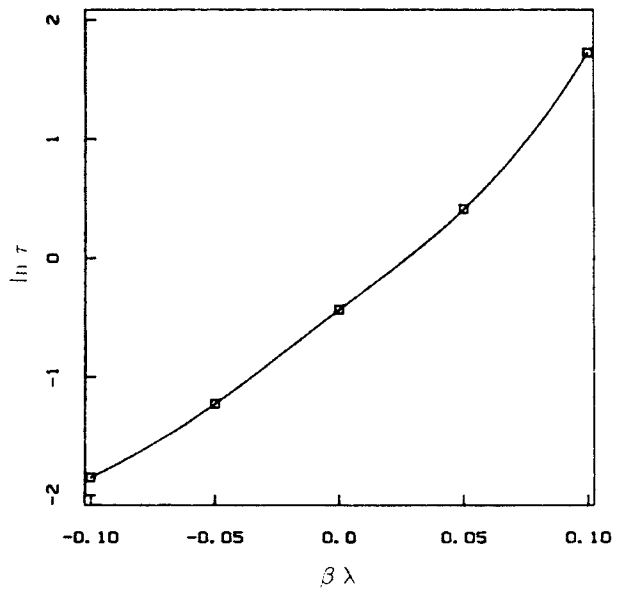

FIG. 12. Arrhenius plot of the average relaxation time for the potential energy. The slope, or activation energy for relaxation, increases as the temperature is lowered.

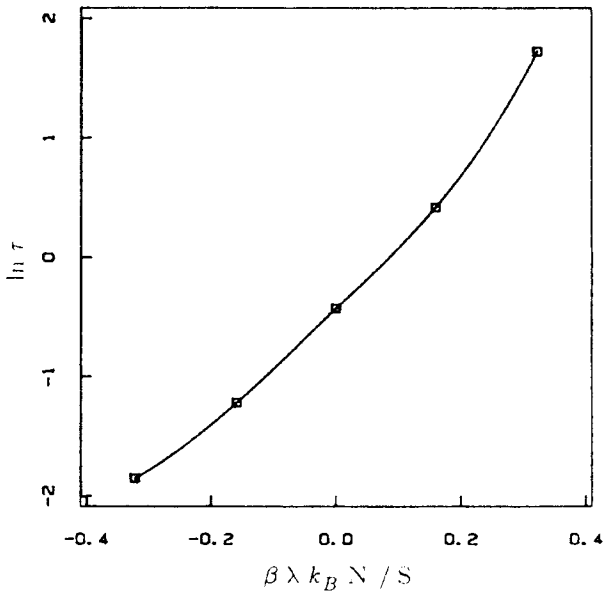

FIG. 13. Adam-Gibbs correlation for the square-tiling model. The average relaxation time for the potential energy is seen to violate the Adam-Gibbs equation, $\log\tau=A+B/TS$, with A and B temperature independent.

states that the activation energy for relaxation in a dense fluid is inversely proportional to the temperature-dependent entropy. To test this hypothesis for the present model we have plotted the logarithm of τ versus $\beta\lambda k_B N/S$ (inversely proportional to TS) in Fig. 13. The curvature in the figure indicates that the Adam-Gibbs hypothesis is not obeyed for the square tiling model. The average relaxation time data in Fig. 12, however, can be accurately fitted with the Vogel-Fulcher equation.

VII. DISCUSSION

The tiling model advocated and investigated in this paper is especially helpful for understanding the behavior of real glasses when it is compared with other precisely defined models. The most obvious case of the latter is provided by the Fredrickson-Andersen facilitated kinetic Ising models.[9–11,25] As we have observed to be the case with the tiling model, the two-spin facilitated model on a square lattice is known from simulation studies[11,25] empirically to exhibit KWW relaxation with variable exponent μ and non-Arrhenius mean relaxation time τ. The model has also been shown to exhibit thermal hysteresis and nonlinear relaxation behavior, and to possess a kinetically unachievable ground-state configuration. However there are some distinctive differences between the tiling model and the two-spin facilitated kinetic Ising model:

(1) Only the tiling model is ergodic (corresponds to an irreducible Markov process), though the large-system-limit properties of the facilitated kinetic Ising model are apparently unaffected by the type of nonergodicity (Markov reducibility) present.[10,11]

(2) The tiling model displays an ideal glass transition,

while the facilitated kinetic Ising model does not.

(3) The two-dimensional two-spin facilitated Ising model accurately obeys the Adam-Gibbs relation, whereas the tiling model shows weak departure therefrom.

(4) The mean tile size offers an obvious equilibrium coherence length in the present model, which in fact would diverge below the ideal glass transition if strict equilibrium obtained. In contrast, no obvious equilibrium coherence length announces its presence in the facilitated Ising model, although it may possess a nonequilibrium "length" associated with the spatial extent of cooperativity.

In view of the fact that both types of models successfully reproduce (at least qualitatively) the principal experimental phenomena, one must eventually ask how many other types could do the same. In other words, how sensitive are these relaxation phenomena to details of available system configurations and of the transition rates between those configurations?

It is probably worth stressing that the tiling models cannot be mapped simply onto spin-$\frac{1}{2}$ Ising models. First of all, it is easy to demonstrate that at least four colors are necessary to color a general configuration of the system, regarded as a "map" with "square countries." Figure 14 shows a specific cluster of six tiles, numbered 1–6 for clarity. Suppose three colors, red (r), yellow (y), and blue (b) would suffice. Then let tiles 1, 2, and 3 in Fig. 14 be arbitrarily assigned the colors r, y, and b as shown. That assignment in turn forces 4 to be r, and 5 to be b. No option among these three colors is then left for tile 6 since it is already bordered by each of the three; QED.

Then since four colors must be employed, each elementary unit of area would have four possible states (colors), indicating a representation of the configurations in terms of a set of spins, equal in magnitude to $\frac{3}{2}$, one attached to each unit of area and thus arranged in a square lattice. Strong and arbitrarily long-ranged many-spin interactions could then be devised to assure that spin components be equal across square domains. However the degree of degeneracy of any such domain pattern with respect to spin changes (map recoloring) would remain a vexing and perhaps unsolvable problem. Alternative strategies that attempt to assign spins to bonds of the original lattice also meet with severe difficulties, in attempting to maintain square domains as the only possible structures.

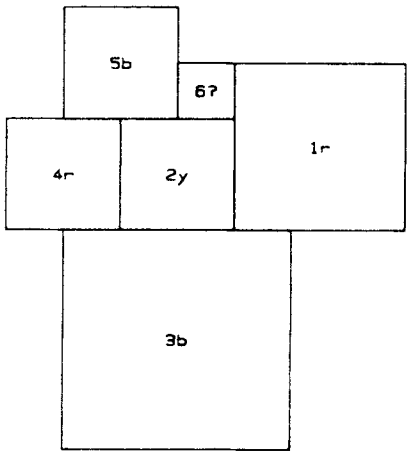

FIG. 14. Tile grouping used to demonstrate the general necessity of using four colors to decorate the "map of square countries."

Finally we mention that an attractive kinetic variant exists for the present tiling model. Instead of the aggregation and fragmentation processes defined in Sec. II that utilize least prime factors, an incremental growth or shrinkage alternative could be invoked, whereby a tile changes its linear dimension by ± 1. This would be accomplished by accreting or shedding an L-shaped group of 1×1's along two contiguous sides. We anticipate that the resulting kinetic behavior would be nontrivially affected, and we are currently initiating the required simulation to evaluate this expectation.

APPENDIX

Equations (2.4) and (2.6) clearly show that fragmentation and aggregation rates for large squares will be very small. Consequently we would expect the long-time asymptotic behavior of equilibrium autocorrelation functions to be dominated by processes involving large squares.

At temperatures above the ideal transition point, the equilibrium concentrations of squares of size $j\times j$ should decrease monotonically according to the expression[16]

$$n_j/N=\exp[-Kj^2-Lj+O(1)],\quad K,L>0\,. \tag{A1}$$

The first two terms explicitly shown in the exponent refer to interior (area) and to perimeter (length) free energies for the medium in which the square is inserted. As temperature is lowered to the transition point, the positive constant K will continuously decrease, becoming zero just at the transition. This criterion is an obvious reflection of the instability that underlies the transition itself: The free energy cost of expelling boundary from a macroscopic region in the system has gone to zero. At any temperature the equilibrium concentration n_j/N for large j represents a dynamic balance between net rate of creation (primarily by aggregation of smaller squares) and rate of destruction (primarily by fragmentation).

Large squares of prime-number size $p\times p$ should be especially long lived. The conceptually simple fragmentation process is especially slow because of the large amount of boundary that must be inserted to create p^2 1×1's, with a correspondingly small Boltzmann factor. The net rate of production must likewise be slow to maintain the equilibrium concentration given by Eq. (A1).

It seems plausible therefore to assume that long-time relaxation will be dominated principally by large squares of prime-number size. The correct qualitative behavior then should emerge from a sum over all prime numbers of a characteristic decay contribution for each prime number p. Representing that sum as an integral (appropriate for large p), we therefore consider the following idealized de-

cay function:

$$f(t)=\int_{p_0}^{\infty} dp(\ln p)^{-1}\exp(-Kp^2-Lp) \times\exp\{-\nu_0 t\exp[-2p(p-1)(\beta\lambda-\ln\alpha)]\} . \quad \text{(A2)}$$

In this expression the successive integrand factors are (i) the asymptotic density of primes among the positive integers,[26] (ii) the p variation of the concentration expression, Eq. (A1); and (iii) a decaying exponential associated with the fragmentation rate for $p\times p$'s. The fixed lower limit p_0 on the integral is irrelevant for present purposes, since asymptotic long time persistence will be associated with asymptotically the largest available prime-number squares. By invoking only the simple fragmentation process in Eq. (A2) we are implicitly supposing that by detailed balance the more complex aggregation processes producing $p\times p$'s will at most only contribute equivalent relaxation times to the overall relaxation spectrum. Thus Eq. (A2) should suffice for our present qualitative purposes.

In the long-time limit, the decay of $f(t)$ can be identified by a saddle-point method. This requires locating the maximum of the integrand as a function of t. Hence we need to minimize the following expression with respect to p:

$$I=\ln\ln p+Kp^2+Lp+\nu_0 t \times\exp[-2p(p-1)(\beta\lambda-\ln\alpha)] , \quad \text{(A3)}$$

which will be achieved, say, at $p_m(t)$. This expression makes it clear that when $K>0$ (i.e., above the transition temperature), $p_m(t)$ will increase to infinity as t increases to infinity. For that limit it suffices to consider a simplified form of expression (A3) (which merely drops subdominant terms):

$$I=Kp^2+\nu_0 t\exp[-2p^2(\beta\lambda-\ln\alpha)] . \quad \text{(A4)}$$

Carrying out the differentiation, we find

$$p_m^2(t)=[2(\beta\lambda-\ln\alpha)]^{-1}\ln[2\nu_0 t(\beta\lambda-\ln\alpha)/K] . \quad \text{(A5)}$$

To evaluate f to leading order at large t, it suffices simply to evaluate the integrand at $p_m(t)$. To be consistent it is necessary to utilize the replacement of (A3) by (A4) in Eq. (A2), with the result:

$$f(t)\cong[(2\nu_0 e/K)(\beta\lambda-\ln\alpha)t]^{-K/[2(\beta\lambda-\ln\alpha)]} . \quad \text{(A6)}$$

Hence we predict an algebraic decay asymptotically. The negative power of t involved is clearly temperature dependent, and goes continuously to zero at the transition point on account of the similar behavior of K in the exponent in Eq. (A6).

Just at the transition point Eq. (A4) must be modified to

$$I=Lp+\nu_0 t\exp[-2p^2(\beta_c\lambda-\ln\alpha)] . \quad \text{(A7)}$$

The analog of Eq. (A5) is an asymptotic series with the following leading term:

$$p_m^2(t)=[2(\beta_c\lambda-\ln\alpha)]^{-1}\ln[(4\nu_0 t p_m/L)(\beta_c\lambda-\ln\alpha)] =[2(\beta_c\lambda-\ln\alpha)]^{-1}\{\ln[(4\nu_0 t/L)(\beta_c\lambda-\ln\alpha)] +\tfrac{1}{2}\ln\ln t+\cdots\} . \quad \text{(A8)}$$

As a result one obtains at the transition point:

$$f(t)\cong\exp\{-L[2(\beta_c\lambda-\ln\alpha)]^{-1/2}(\ln t)^{1/2}\} , \quad \text{(A9)}$$

a function which declines to zero with increasing t more slowly than any inverse power.

[1]H. Rawson, *Properties and Applications of Glasses* (Elsevier, Amsterdam, 1980).
[2]G. Adam and J. H. Gibbs, J. Chem. Phys. **43**, 139 (1965).
[3]M. H. Cohen and G. S. Grest, Phys. Rev. B **20**, 1077 (1979); **21**, 4113 (1980).
[4]E. Leutheusser, Phys. Rev. A **29**, 2765 (1984).
[5]S. P. Das, G. F. Mazenko, S. Ramaswamy, and J. J. Toner, Phys. Rev. Lett. **54**, 118 (1985).
[6]T. R. Kirkpatrick, Phys. Rev. A **31**, 939 (1985).
[7]J. J. Ullo and S. Yip, Phys. Rev. Lett. **54**, 1509 (1985).
[8]U. Bengtzelius, W. Göetze, and A. Sjölander, J. Phys. C **17**, 5915 (1984).
[9]G. H. Fredrickson and H. C. Andersen, Phys. Rev. Lett. **53**, 1244 (1984).
[10]G. H. Fredrickson and H. C. Andersen, J. Chem. Phys. **83**, 5822 (1985).
[11]G. H. Fredrickson and S. A. Brawer, J. Chem. Phys. **84**, 3351 (1986).
[12]O. S. Narayanaswamy, J. Am. Ceram. Soc. **54**, 491 (1971).
[13]C. T. Moynihan, P. B. Macedo, C. J. Montrose, P. K. Gupta, M. A. DeBill, B. E. Dow, P. W. Drake, A. J. Easteal, P. B. Elterman, R. P. Moeller, H. Sasabe, and J. A. Wilder, Ann. N.Y. Acad. Sci. **279**, 15 (1976).
[14]A. J. Kovacs, Ann. N.Y. Acad. Sci. **371**, 21 (1981).
[15]G. W. Scherer, J. Am. Ceram. Soc. **67**, 504 (1984).
[16]F. H. Stillinger and T. A. Weber, Ann. N.Y. Acad. Sci. (to be published).
[17]F. H. Stillinger and T. A. Weber, Science **225**, 983 (1984).
[18]F. H. Stillinger and R. A. LaViolette, Phys. Rev. B **34**, 5136 (1986).
[19]D. Shechtman, I. Blech, D. Gratias, and J. W. Cahn, Phys. Rev. Lett. **53**, 1951 (1984).
[20]N. Metropolis, A. W. Metropolis, M. N. Rosenbluth, A. H. Teller, and E. Teller, J. Chem. Phys. **21**, 1087 (1953).
[21]A. B. Bortz, M. H. Kalos, and J. L. Lebowitz, J. Comp. Phys. **17**, 10 (1975).
[22]G. A. Baker, Jr., J. L. Gammel, and J. G. Wills, J. Math. Anal. Appl. **2**, 21 (1961); **2**, 405 (1961).
[23]S. Brawer, J. Chem. Phys. **81**, 954 (1984).
[24]A. K. Jonscher, Nature **267**, 673 (1977).
[25]G. H. Fredrickson, Ann. N.Y. Acad. Sci. (to be published).
[26]A. E. Inghan, *The Distribution of Prime Numbers*, Vol. 30 of *Cambridge Tracts in Mathematics and Mathematical Physics* (Cambridge University Press, Cambridge, 1932), p. 3.